Development of detector pixels based on silicon photomultipliers for the Cherenkov gamma-ray telescope TAIGA-IACT

A A Bogdanov[1], Yu V Tuboltsev[1], Yu V Chichagov[1] and A M Krassilchtchikov[1]

[1] Ioffe Institute, St. Petersburg, 194021 Russia

E-mail: Alexander.A.Bogdanov@mail.ioffe.ru

Abstract. The design and scheme of signal readout from silicon photomultipliers OnSemi MicroFJ-60035 used as sensitive elements (pixels) of a new detector cluster for the camera of the Cherenkov gamma-ray telescope TAIGA-IACT are developed. The design of the developed pixel follows the shape of the photomultiplier tube XP1911 using in the first generation clusters, and that provides compatibility of the new cluster with the telescope camera. Due to the adjustable gain, the developed scheme allows one to detect and digitize signals in a wide dynamic range from several to 10 000 photons.

1. Introduction

Currently at the Ioffe Institute (Russia) development of a new detector cluster for the camera of the Cherenkov gamma-ray telescope TAIGA-IACT [1, 2] with detector elements based on silicon photomultipliers (SiPM) OnSemi MicroFJ-60035 sensitive both to visible (250-600 nm) and ultraviolet (250-300 nm) radiation [3] is in progress. The primary aim of the TAIGA observatory is to study both steady and transient space sources of TeV-range gamma-rays as well as to measure the spectrum of cosmic rays from tens of TeV to tens of PeV including the important “knee” region usually associated with a transition from galactic to extragalactic sources of cosmic rays [4]. The development of a new detector cluster is based on numerical modeling made by the authors and on the experience of creating test boards for registration of photons by silicon photomultipliers (SiPM) on a specially designed test bench [5]. The preparatory work made it possible to move on to the next important stage in creation of a new detector cluster – design of its structure and circuitry. As an important part of this task, a number of signal readout schemes with SiPMs differing from each other in a number of parameters, such as gain, bandwidth, power consumption, heat dissipation, and operating range were created. This article is devoted to the description of the best of the developed schemes of the detector pixel.

2. The pixel structure and design

The detector cluster is being developed for use in the existing telescope camera TAIGA-IACT, and this imposes a number of restrictions on its design and circuitry. An important feature of the new cluster is its complete interchangeability with the existing cluster based on vacuum photomultipliers (PMT) XP1911. These vacuum photomultipliers, which are the basis of the current camera, have a cylindrical shape with a detecting plane at the end; this means that the developed pixel must have a similar cylindrical body for compatibility with existing camera components. Since silicon

photomultipliers SiPM are produced in a relatively small square shape, it was decided to use 4 detectors OnSemi MicroFJ-60035 in order to achieve a detector area coverage similar to that of PMT XP1911. This allows one not to make significant changes in the design of optical concentrators used in TAIGA-IACT (hexagonal Winston cones).

Let's consider the design features of the developed pixels, since these features also affect the circuit design solutions.

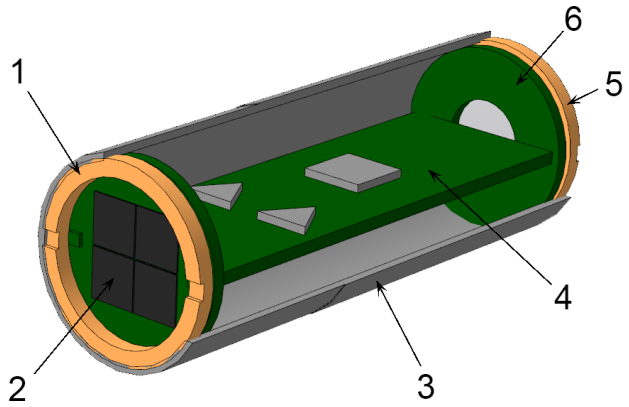

Figure 1. A section view of the new detector pixel. 1 and 5 - pressure rings with external thread, 2 – the detector board, 3 – housing (in the section), 4 – the preamplifier board, 6 – the rear board.

Figure 1 shows the view of the pixel followed the shape of the photomultiplier PMT XP1911. The detector board is a round printed circuit board with a diameter of 25 mm, which contains four SiPMs. The preamplifier board is located perpendicular to it. Together they are placed inside a cylindrical aluminum housing and are fixed with pressure rings. This design solution is necessary for placing the readout electronics in the immediate vicinity of the signal source – SiPM. However, the transmission of a weak signal from the detector board to the preamplifier board creates problems such as signal degradation while transmission, and difficulty of structure assembly and disassembly. Experiments with other versions of the readout schemes with the signal transmission from the detectors board to the preamplifier board via a multi-pin connector DS1065-14-2X14S8BR showed that the quality of the transmitted signal noticeably decreases. Therefore, it was decided to connect both boards in a permanent joint by soldering boards at the right angle.

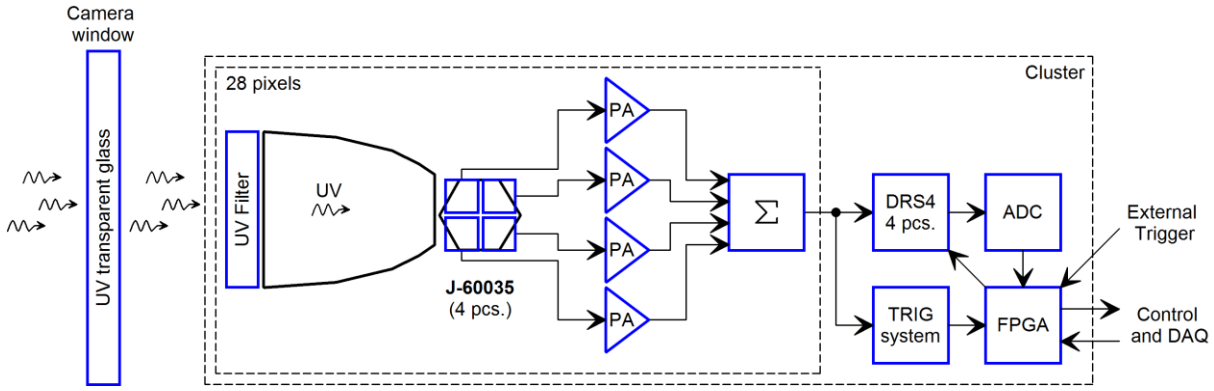

Figure 2. The schematic diagram of the detector cluster.

Let's consider the schematic diagram of the developed cluster containing 28 sensitive elements – pixels (Figure 2). The photons recorded by the telescope pass through the entrance window of the

telescope camera, the optional UV filter and the concentrator (a hexagonal Winston cone) and hit one of the four SiPM MicroFJ-60035 detectors in the pixel. The signal generated by the detectors is amplified by preamplifiers, summed up and transmitted from the pixel to the analog memory chip DRS4 [6] and to the trigger system, which determines whether a given signal should be treated as a true source signal by the number of pixels triggered in the cluster and their relative positions. If the signal is considered as source, a trigger pulse is generated on the logic chips (collectively designated as FPGA). After some time required to record the entire source signal to the DRS4 memory, FPGA sends a stop pulse to DRS4 and begins the procedure of digitizing the source signals using the analog-to-digital converter (ADC). After digitization, FPGA has the digitized signal from the pixel and the pulse amplitude in memory, and then this data can be read out by the external data acquisition system of the telescope.

3. The readout scheme

The source signal that the cluster pixels should register, has two ranges depending on the wavelength. Taking into account the overall detection efficiency, the source signal is expected to be from several to several tens of photons in the ultraviolet range (250 – 300 nm) observed with dedicated ultraviolet filters, and from hundreds to several thousand photons in the visible range (250 – 600 nm). For better separation of the source signal from the dark count pulses and from the night sky background photons, the pulses of the source signal must have a minimum duration. The fast output of the MicroFJ-60035 detector with the use of an appropriate signal readout scheme allows one to achieve a pulse full width at half maximum less than 10 ns. Let's consider the selected signal readout scheme for the MicroFJ-60035, which has the best characteristics of several schemes we considered, developed and tested (Figure 3).

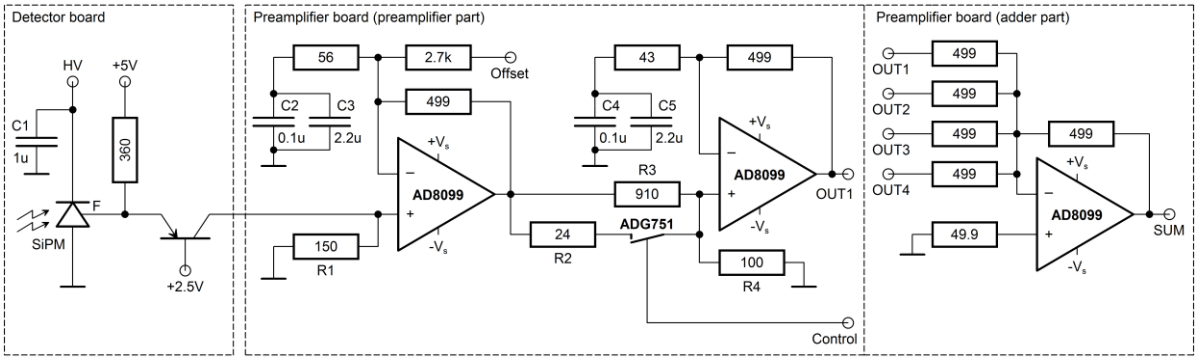

Figure 3. The scheme of the signal readout from the detector pixel.

The signal readout scheme consists of three parts: the detector board, the dual-stage preamplifier and the adder. A current follower based on the BFT93 wideband low-noise transistor is located on the detector board. The signal from BFT93 is transmitted via a soldered connection between the boards to the first stage of the preamplifier based on the AD8099 wideband low-noise operational amplifier. This signal readout scheme provides amplification and conversion of the current from the detector fast output to voltage with transimpedance 1500 Ω and bandwidth greater than 200 MHz. It is noteworthy that the first stage has a gain factor $k = 8.9$ only for high frequencies, but for direct current (DC) the amplifier operates as DC follower, due to capacitors C2 and C3 separating the inverting input of the amplifier from the ground ($k = 1$). Additionally, the inverting input of the amplifier is connected to the offset voltage input, which allows to compensate the constant offset level of 0.75 V formed on the non-inverting input of the amplifier by the direct current flowing through the transistor and resistance R1 (150 Ω).

The second stage of the preamplifier is also based on AD8099 in a similar high-frequency gain scheme with the use of capacitors C4 and C5. However, since the wide dynamic range of the input

signals (from several to 10 000 photons) is required, the ADG751 switch was added to the scheme allowing to bypass the resistor R3 (910 Ω) in the voltage divider R3-R4 at the non-inverting input of the second stage. In order to minimize the influence of the switch parasitic capacitance, the resistor R2 (24 Ω) was inserted. Assume that the case with the opened switch corresponds to the non-amplified mode ($k = 1$), then the case with the closed switch corresponds to $k = 7.2$. Actually the measured amplification factor between these modes was slightly greater ($k = 8.4$), this can be explained by scattering of the resistance value of the resistors and the switch.

The last amplifier AD8099 operates as an adder of the four signals from four SiPMs. The full width at half maximum of the output is 3.5 ± 0.7 ns. The power consumption of the developed pixel is about 1.5 W.

4. Operation range of the pixel

In order to determine the operation range of the developed pixel, tests were carried out using the pulsed ultraviolet radiation source PicoQuant PLS-270 capable to emit light pulses at the wavelength of 277 nm and of 600 ps duration. The source was connected to the pixel by a black rubber corrugation providing the light insulated volume and the ability to adjust the distance to the source. The output signal from the pixel was recorded by the oscilloscope LeCroy WaveRunner 620Zi with the bandwidth of 2 GHz in a DC50 mode.

The pixel operation range in voltage units is determined by amplifiers and their power supply voltages. Assume that upper limit of the range (the maximum possible signal) is equal to 3000 mV, then the signal of such amplitude will not be affected by nonlinear distortions from the amplifier. The lower range limit may be set to 100 mV. Then for conversion of the operating range from the voltage unit into the units of registered photons, an accounting detector overvoltage is needed. In order to perform such conversion, it is necessary to determine the value of the single signal. The single signal (or 1 photoelectron – 1 ph.e.) below refers to a signal from a single microcell of a silicon photomultiplier, induced by either a dark count or a photon hit event. The amplitude of the single signal can be defined as a difference between the amplitudes of the 2 ph.e. and 1 ph.e. signals For example, at the detector overvoltage of 4.5 V, the single signal for the considered scheme with amplification (the switch is closed) is 32.7 ± 4.5 mV, and 3.8 ± 0.7 mV without amplification (the switch is opened). However, the value of the single signal strongly depends on the overvoltage of the detector. This fact on one hand allows to significantly expand the operating range of the detected photons, and on another hand, makes the conversion from voltage to photoelectrons more difficult. Therefore it is required to make a calibration table of the dependence of the value of the single signal on the detector overvoltage.

Direct measurements of a single signal are not always possible especially for small single signals at low overvoltage. Therefore, the following method was used to make the calibration table. The photon source was set up at such distance and adjusted to such intensity that at the maximum detector overvoltage (6 V) there was a maximum possible output signal (3 V) for the pixel. Further, with a gradual decrease in the overvoltage down to a minimum overvoltage (1 V), the signal amplitude from the pixel was measured. The ratio between the measured values of the signal amplitude and the average number of registered photons gives the dependence of the single signal value on the detector overvoltage (Fig. 4). The average number of the registered photons can be obtained using a radiation power meter at determination of the photo-detection efficiency (PDE) of the silicon photomultiplier. The method is described in more detail in [7].

The approximation error of the linear part (overvoltage 1.5 − 5.3 V) of the dependence in Figure 4 is 3.1%. The deviation of the dependence from linear at higher overvoltage corresponds to saturation of the amplifiers (the signal higher than 3 V), and at lower overvoltage the nonlinearity corresponds to decreasing the signal-to-noise ratio and increasing the influence of the self noise of the amplification path. Dividing the selected upper and lower signal limits by the single signal for each overvoltage it is possible to obtain the operation range of the pixel for each gain mode (Figure 5).

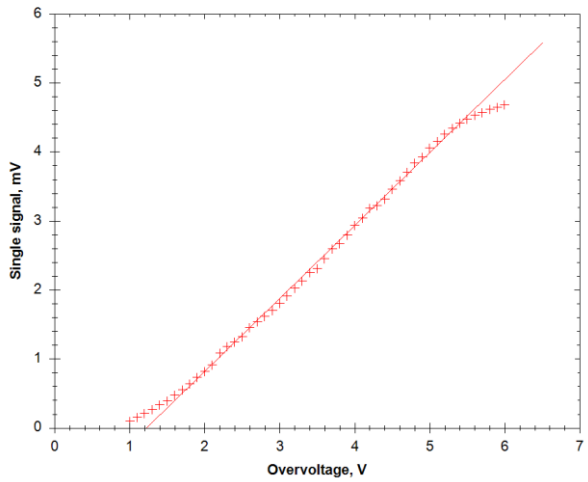

Figure 4. The dependence of the value of the single signal on the detector overvoltage for the mode without amplification. The linear approximation of the main part of the dependence is shown.

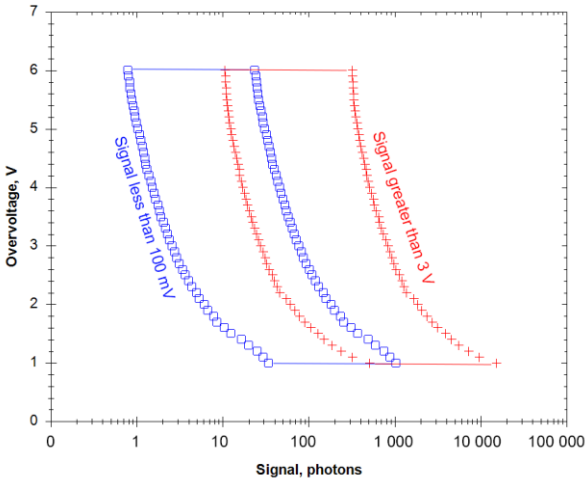

Figure 5. Operation ranges of the pixel with amplification (blue squares) and without amplification (red pluses).

5. Conclusion

A new design of pixel detector for the Cherenkov gamma-ray telescope TAIGA-IACT has been developed. The design will allow one to install the detector cluster, consisting of the developed pixels, to the existing camera of the Cherenkov gamma-ray telescope TAIGA-IACT without a need for any telescope construction changes. A scheme for signal readout from silicon photomultipliers providing detection of signals from several to 10 000 photons by a switchable amplification factor and a detector overvoltage control has been developed. However, the overall pixel power consumption remains relatively high (1.5 W), and that will probably require further improvements in order to reduce the power consumption, such as reduction of the number of amplifiers by summing the signals right after the first amplification stage or making specific design changes to improve heat dissipation from the microchips to the aluminum housing.

Acknowledgements

This research has been supported by RSF via grant 19-72-20045.

References

[1] Kuzmichev L A *et al.* 2018 TAIGA Gamma Observatory: Status and Prospects *Physics of Atomic Nuclei* **81** 4 497-507
[2] Budnev N M *et al.* 2019 TAIGA: a complex of hybrid systems of cooperating detectors for gamma astronomy and cosmic ray physics in the Tunka valley *Bulletin of the Russian Academy of Sciences: Physics* **83** (8) 951–4
[3] OnSemi J-Series SiPM Sensors Datasheet https://www.onsemi.com/pub/Collateral/MICROJ-SERIES-D.PDF
[4] Kulikov G V and Khristiansen G B 1958 On the size distribution of extensive atmospheric showers *Zh. Eksp. Teor. Fiz.* **25** 635
[5] Bogdanov A A *et al.* 2020 Modelling of SiPM performance for detection of cherenkov radiation from extensive air showers in UV and visible ranges for application at the TAIGA-IACT telescope *Latvian Journal of Physics and Technical Sciences* ***57*** (1-2) 13-21
[6] The Paul Scherrer Institute, DRS Chip Home Page https://www.psi.ch/en/drs

[7] Bogdanov A A *et al.* 2020 Measurements of the 277 nm photon detection efficiency of the OnSemi MicroFJ-60035 silicon photomultiplier *J. Phys.: Conf. Ser.* **1697** 012015